

## Supporting Information

### **Localized Electron Density Modulation in Conjugated Polymer Nanosheet for Boosting Photocatalytic H<sub>2</sub> evolution**

Yaoyao Liu, Haifeng Yu, Chong Shi and Zhonghua Xiang\*

Beijing Advanced Innovation Center for Soft Matter Science and Engineering, State Key Laboratory of Organic-Inorganic Composites, College of Chemical Engineering, College of Energy, Beijing University of Chemical Technology, Beijing 100029, P. R. China

E-mail: [xiangzh@mail.buct.edu.cn](mailto:xiangzh@mail.buct.edu.cn)

### **Table of Contents**

1. Experimental section.....	S1
1.1 Materials.....	S1
1.2 Synthesis of COP-PB-N2.....	S1
2. Characterizations.....	S2
2.1 Materials characterization.....	S2
2.2 Photoelectrochemical test.....	S2
2.3 Photocatalytic test.....	S3
2.4 Apparent Quantum Yield (AQY) Measurement.....	S3
2.5 Theoretical calculation.....	S4
3. Supplementary Figures and Tables.....	S5
4. References.....	S19

## 1. Experimental section

### 1.1 Materials

All chemical reagents were purchased from commercial source. 1,4-Phenylenebisboronic acid, Tetrakis (triphenylphosphine) palladium [Pd(PPh<sub>3</sub>)<sub>4</sub>], triethylamine, methanol, and N, N-dimethylformamide (DMF) were purchased from J&K. 2,7-Dibromophenanthrene and 3, 8-Dibromophenanthroline were obtained from Bidepharm. Potassium carbonate (K<sub>2</sub>CO<sub>3</sub>) and hydrochloric acid were obtained from Beijing Chemical Works.

### 1.2 Synthesis of COP-PB-N2 and COP-PB

0.5 mmol 3, 8-Dibromophenanthroline and 0.5 mmol 1,4-Phenylenebisboronic acid were dispersed into N, N-dimethylformamide (50 ml) with round-bottom flask via ultrasonic treatment for a while. Then, the above mixture was bubbled by nitrogen (N<sub>2</sub>) for 30 minutes. The Pd(PPh<sub>3</sub>)<sub>4</sub> (40 mg) was added into the above solution under N<sub>2</sub> atmosphere and stirred for 30 minutes, after that the aqueous K<sub>2</sub>CO<sub>3</sub> (8 mL, 2.0 M) was added into the mixture. The above reactant would be heated at 150 °C for 2 days. During the reaction, the reaction solution was bubbled by N<sub>2</sub> all the time. When the solution was cooled down to the room temperature, it would be transferred into water (150 ml). The product was obtained by filtration and washed with H<sub>2</sub>O, methanol and tetrahydrofuran. The precipitate was dried at 80 °C overnight. Then, the corresponding polymers were dispersed in 200 ml N-Methyl pyrrolidone (NMP), which was subjected to ultrasonication for 2 hours (100 W, 40 kHz) at room temperature. The product was collected by filtration and washed with H<sub>2</sub>O and methanol and dried under vacuum at 80 °C overnight. The product was obtained as 101 mg, and the yield was 79.5 %. The COP-PB was synthesized by the similar method except the usage of monomer: 2,7-Dibromophenanthrene and 1,4-Phenylenebisboronic acid. The product was obtained as 103 mg, and the yield was 81.7 %.

## **2. Characterizations**

### **2.1 Materials characterization.**

The disappeared functional groups of  $-B(OH)_2$  and  $-Br$  were monitored via Fourier transform infrared spectroscopy (FT-IR, Bruker Vertex 70 V, Germany). The formation of new C-C bonds was measured by  $^{13}C$  solid-state nuclear magnetic resonance spectra (NMR, Bruker AV300, Switzerland). The UV-vis diffuse reflectance spectra of polymers was performed in the solid state on a TU-1901 spectrophotometer. The crystallization property of covalent organic polymers was assessed through Powder X-ray diffraction (PXRD, D/Max 2000 diffractometer, Bruker D2 PHASER, Germany). The X-ray photoelectron spectroscopy (XPS, Thermo Scientific ESCALAB 250, American) was carried out to investigate the surface chemical states of as-synthesized polymers. The transmission electron microscopic (TEM, Hitachi 7700, Japan) was implemented to reveal the morphology of as-prepared covalent organic polymers. The thickness of those polymers was measured by the Atomic Force Microscopy (AFM, SPA-400, Japan). The photo-excited electron-holes were detected by Electron Paramagnetic Resonance (EPR, Bruker 500, Germany) assisted with TEMPO (2,2,6,6-Tetramethylpiperidinoxy). The water wettability was performed by contact angle meter (OCA15Pro, Dataphysics). Time-resolved transient PL decay spectra was measured via Lifetime and Steady State Spectrometer (FLS 980) at room temperature. Ultraviolet photoelectron spectroscopy (UPS) was measured with a monochromatic He I light source (21.2 eV) and Spherical Analyzer via PHI5000 VersaProbe III.

### **2.2 Photoelectrochemical test**

The working electrode was assembled based on previous report.<sup>1</sup> Typically, 1 mg as-synthesized polymers and 4 ml ethanol were mixed together and ultrasonically dispersed for 30 min. Meantime, the fluorine-doped tin oxide (FTO) glasses were washed by acetone, deionized water and anhydrous ethanol, respectively. Then, the photocatalyst was uniformly spread on

the FTO glass via drip coating method. The working electrode was subsequently dried at 70 °C for 2 h in a vacuum oven. In addition, the photocurrent response, electrochemical impedance spectra (EIS) and Mott–Schottky plots were carried out via three electrode system (FTO as working electrode; Platinum sheet as counter electrode; saturated calomel as reference electrode) on CHI 600 workstation using 0.2 M Na<sub>2</sub>SO<sub>4</sub> aqueous solution.

### 2.3 Photocatalytic test.

The visible-light-driven H<sub>2</sub> production rate of polymers was evaluated on the basis of our previous method.<sup>2</sup> 5 mg polymer photocatalyst COP-PB-N2 (COP-PB) was uniformly dispersed into 20 ml deionized water containing 2 ml methanol and 2 ml triethylamine (TEA). Then, the above solution was transferred into 60 ml quartz tube. Before visible light ( $\lambda \geq 400$  nm) irradiation, the quartz tube was bubbled with nitrogen for 30 minutes. In the end, the produced H<sub>2</sub> was detected by gas chromatography (GC). As to photocatalytic cyclic test, the produced H<sub>2</sub> was detected every hour. After four hours reaction, the reaction quartz tube was degassed with nitrogen for 30 minutes. Then, the quartz tube was irradiated under visible light and the H<sub>2</sub> was detected every hour again.

### 2.4 Apparent Quantum Yield (AQY) Measurement

The apparent quantum yield (AQY) was evaluated via previous method at different monochromatic light.<sup>2</sup> After photocatalytic hydrogen evolution reaction for one hour, the amount of H<sub>2</sub> was detected via gas chromatography (GC). The AQY was calculated based on the equation as below:

$$\text{AQY} = \frac{Ne}{N_p} \times 100\% = \frac{2 \times N \times N_A \times h \times c}{S \times P \times t \times \lambda} \times 100\%$$

$N$  is the amount of hydrogen molecules,  $N_A$  is Avogadro constant,  $c$  is the speed of light,  $h$  is Planck constant,  $t$  is the photocatalytic reaction time,  $\lambda$  is the wavelength of monochromatic light,  $S$  is the irradiation area,  $P$  is monochromatic light intensity.

## 2.5 Theoretical calculation.

The Theoretical calculations based on density functional theory (DFT) were performed via Vienna ab initio simulation package (VASP).<sup>3</sup> The exchange correlation energy was modelled using Perdew–Burke–Ernzerhof (PBE) functional within the generalized gradient approximation (GGA).<sup>4</sup> The Projector-augmented-wave (PAW) potentials were used to describe electron-ion interaction.<sup>5</sup> The cut-off energy of 500 eV was employed for all the calculations, and the Brillouin zone was sampled by the Gamma center k points grids of 1x1x1 and 8x1x1 for structure optimization and electronic structure calculations, respectively. In order to avoid the mutual influence of adjacent periods, a vacuum layer of at least 15 Å was used in the Y- and Z -directions. The convergence threshold for the self-consistent field (SCF) was set at 10<sup>-6</sup> eV and 0.02 eV/ Å for the force of the system converged.

The catalytic hydrogen evolution reaction performance can be evaluated via calculating the reaction free energy( $\Delta G_{H^*}$ ) for hydrogen adsorption, which is determined as follows:

$$\Delta G_{H^*} = \Delta E_{H^*} + \Delta E_{ZPE} - T\Delta S_H$$

The  $\Delta E_{H^*}$  is the adsorption energy calculated by the formula of  $\Delta E_{H^*} = E_{H^*} - E^* - 1/2E_{H_2}$ ,  $\Delta E_{ZPE}$  is the zero-point energy change between the adsorbed state and the gas-phase state of hydrogen from vibrational frequency calculation. The  $\Delta S_H$  is the entropy change which approximate  $1/2(S_{H_2})$  ( $\Delta S_H \approx 1/2(S_{H_2})$ ), where  $S_{H_2}$  is the entropy of gas phase  $H_2$  at standard condition.

### 3. Supplementary Figures and Tables

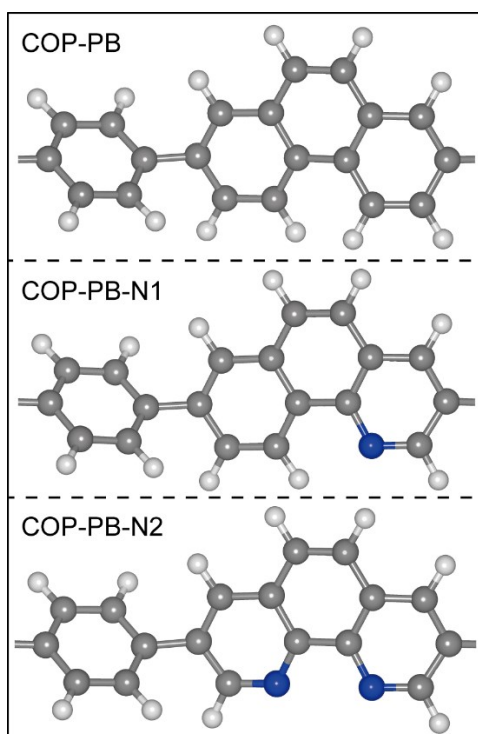


Figure S1. The structure models of COP-PB, COP-PB-N1 and COP-PB-N2.

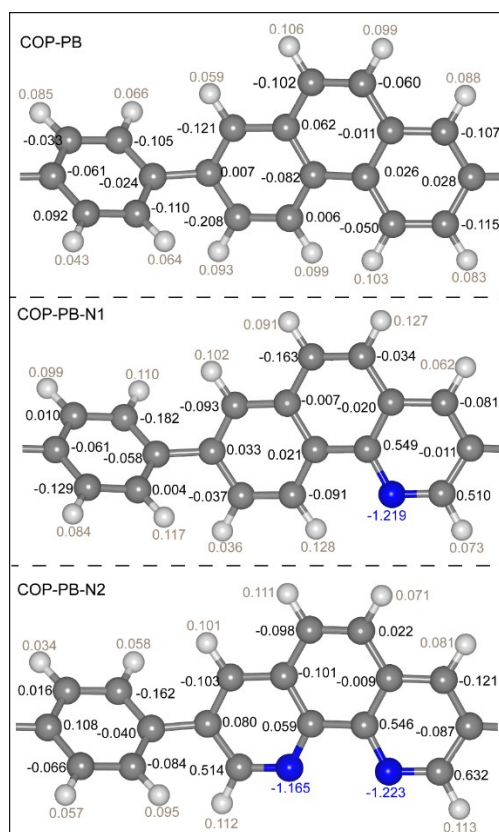


Figure S2. The bader effective charges of COP-PB, COP-PB-N1 and COP-PB-N2.

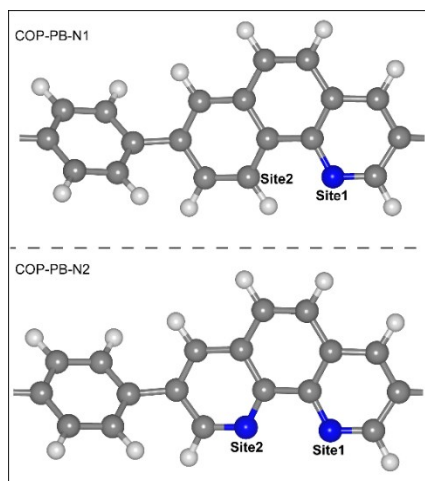


Figure S3. The schematic diagram of labeling site of COP-PB-N1 and COP-PB-N2.

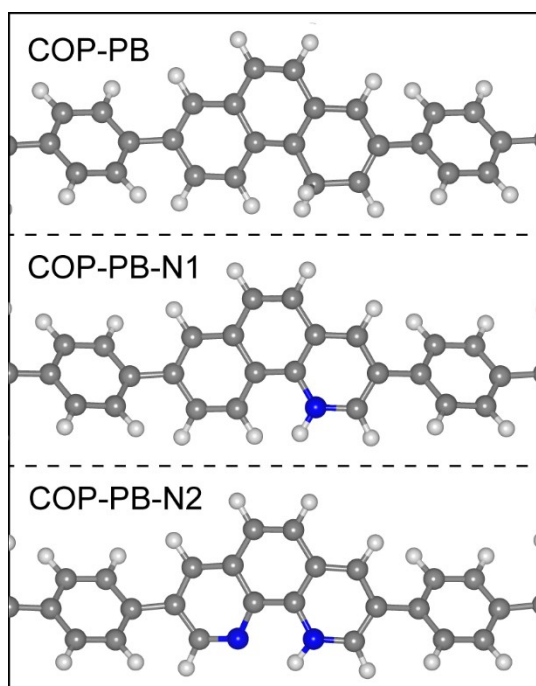


Figure S4. The optimized adsorption structures of three conjugated polymers.

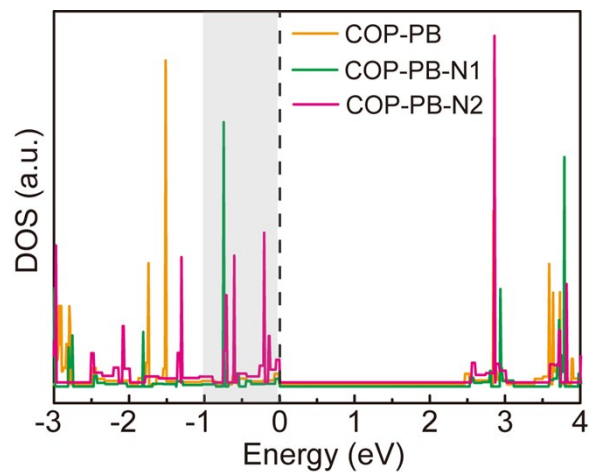


Figure S5. The density of states of COP-PB, COP-PB-N1 and COP-PB-N2.

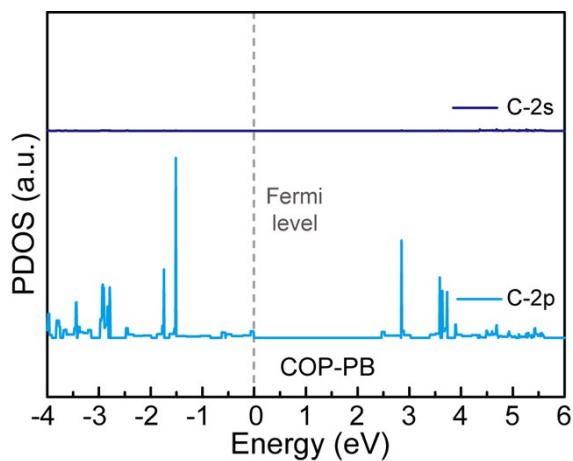


Figure S6. The partial density of states of COP-PB.

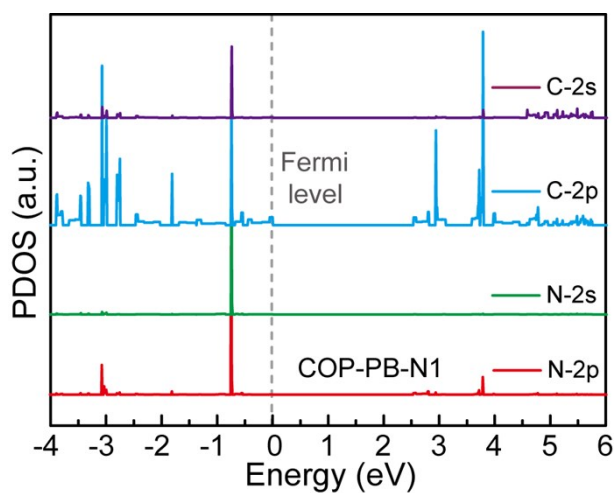


Figure S7. The partial density of states of COP-PB-N1.



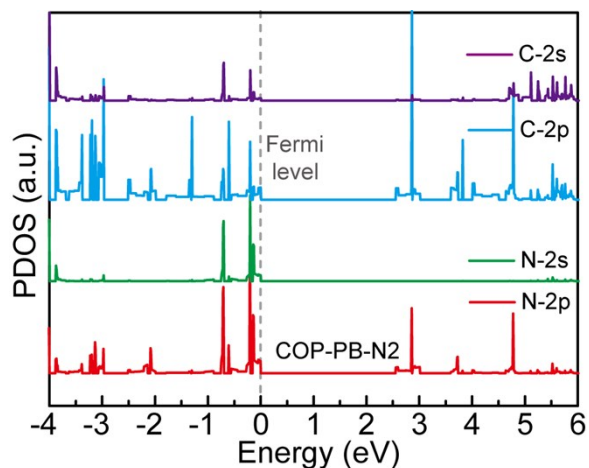


Figure S8. The partial density of states of COP-PB-N2.

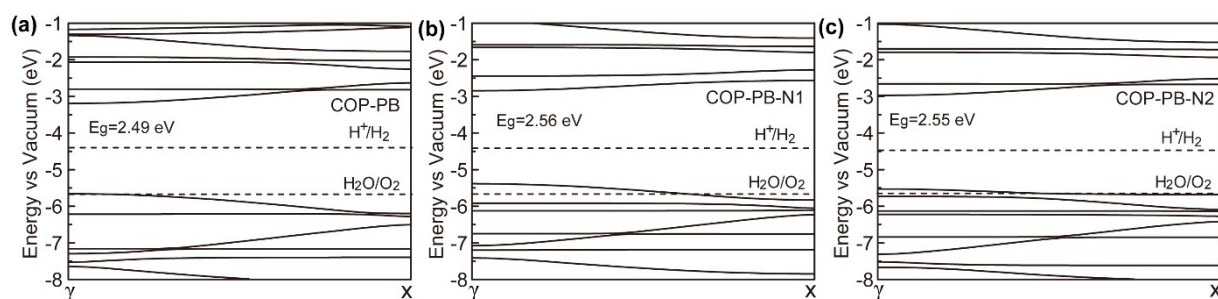


Figure S9. The calculated band structure of as-prepared polymers

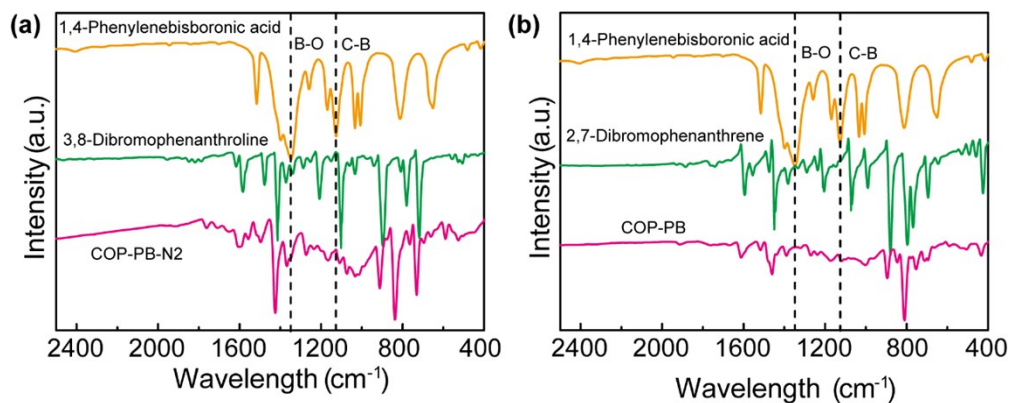


Figure S10. (a) FT-IR spectra of COP-PB-N2, 1,4-Phenylenebisboronic acid and 3, 8-Dibromophenanthroline; (b) FT-IR spectra of 2,7-Dibromophenanthrene, COP-PB and 1,4-Phenylenebisboronic acid. Note: The typical peaks at approximately 1350 and 1125  $\text{cm}^{-1}$  are assigned to the B-O and C-B bonds in the monomers, which are disappeared in the obtained polymers, confirming the successful C-C coupling and synthesis of COP-PB and COP-PB-N2.

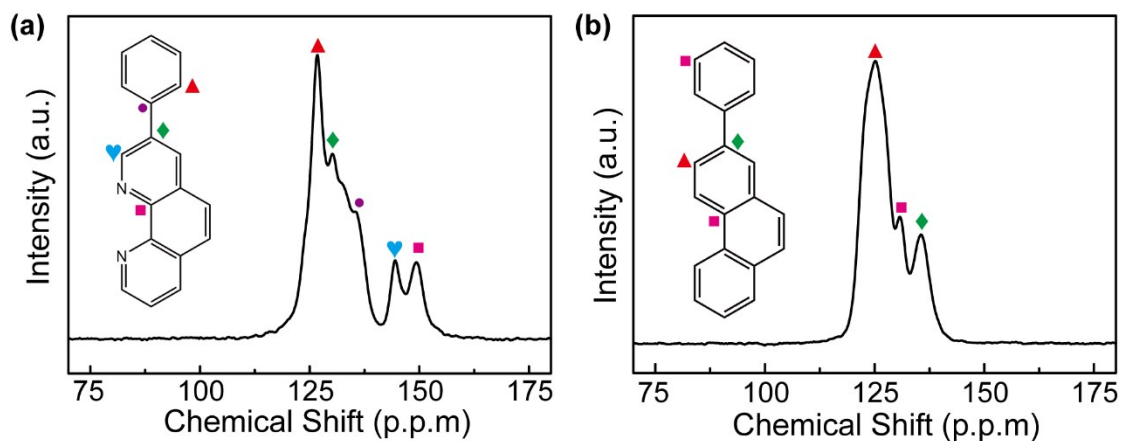


Figure S11.  $^{13}\text{C}$  solid-state nuclear magnetic resonance (NMR) spectra of COP-PB-N2 (a) and COP-PB (b). Note: The two peaks at 144 ppm and 149 ppm in Figure (a) should be attributed to the typical signal of N-containing phenanthroline structure. Moreover, the two figures present the same signal at 135 ppm which is assigned to the newly formed C-C bond, also demonstrating the successful linking of the corresponding two monomers.

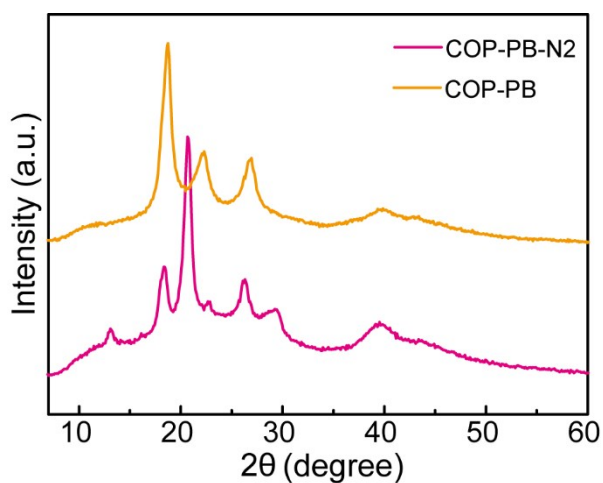


Figure S12. The PXRD patterns of COP-PB-N2 and COP-PB.

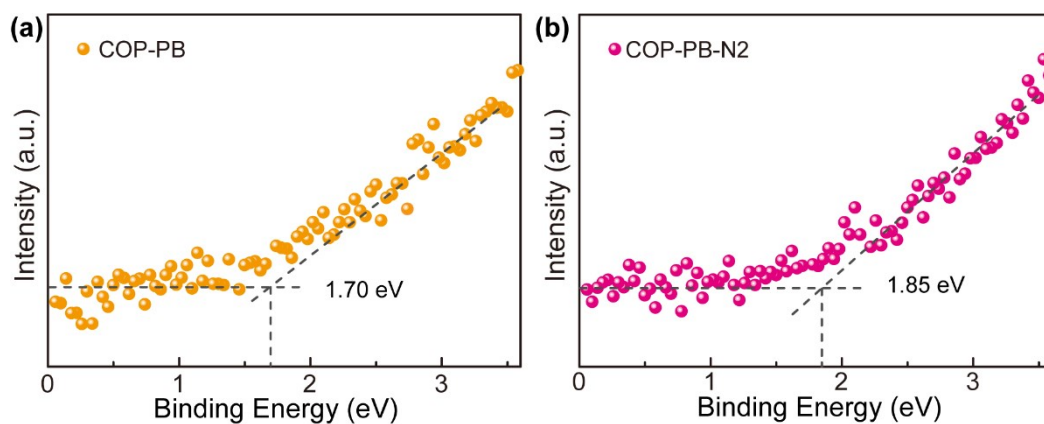


Figure S13. The UPS spectra of valence band for COP-PB and COP-PB-N2.

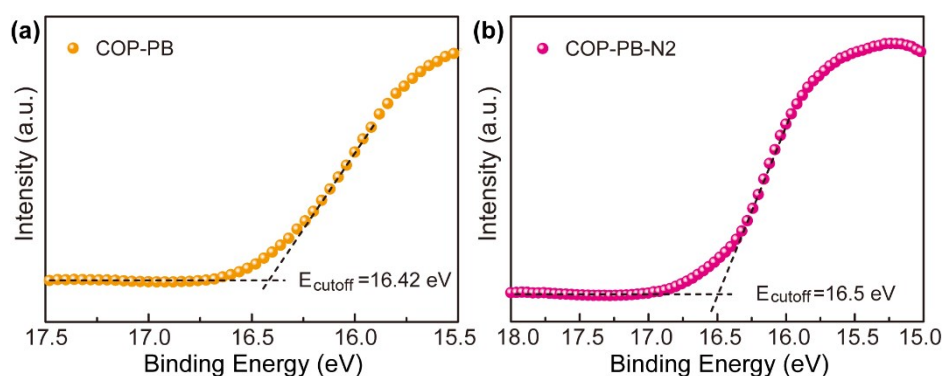


Figure S14. The secondary electron cut-off.

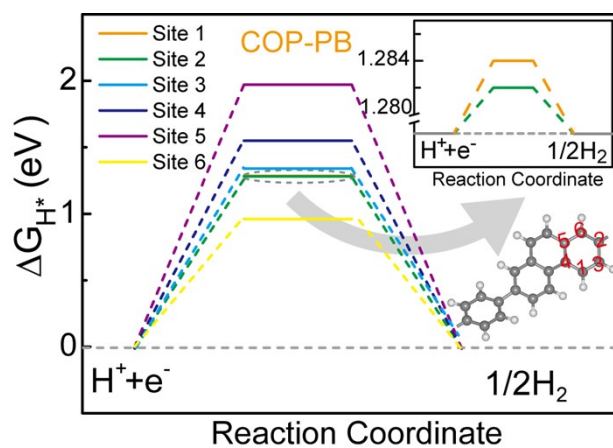


Figure S15. The calculated hydrogen evolution reaction energy profile of different sites (Inset: enlarged image of site 1 and site 2). Note: The  $\Delta G_{H^*}$  has an obvious difference ranging from 0.96 eV to 1.97 eV. The minimum  $\Delta G_{H^*}$  is also relatively far from the optimal value of  $\Delta G_{H^*} = 0$  eV, indicating an inherently low catalytic activity for hydrogen evolution reaction.

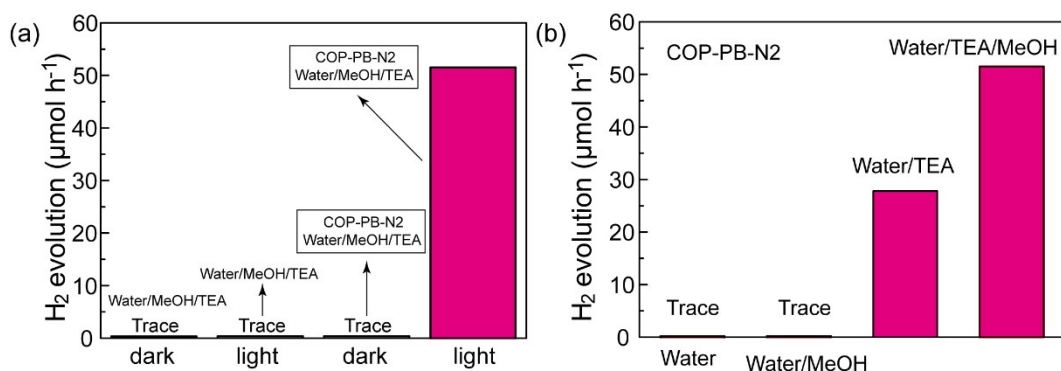


Figure S16. (a) The photocatalytic hydrogen evolution under different conditions: (1) Water/MeOH/TEA mixture in dark; (2) Water/MeOH/TEA mixture in visible light ( $\lambda \geq 400$  nm); (3) COP-PB-N2 with Water/MeOH/TEA in dark; (4) COP-PB-N2 with Water/MeOH/TEA in visible light ( $\lambda \geq 400$  nm). (b) The photocatalytic hydrogen evolution under visible light ( $\lambda \geq 400$  nm).

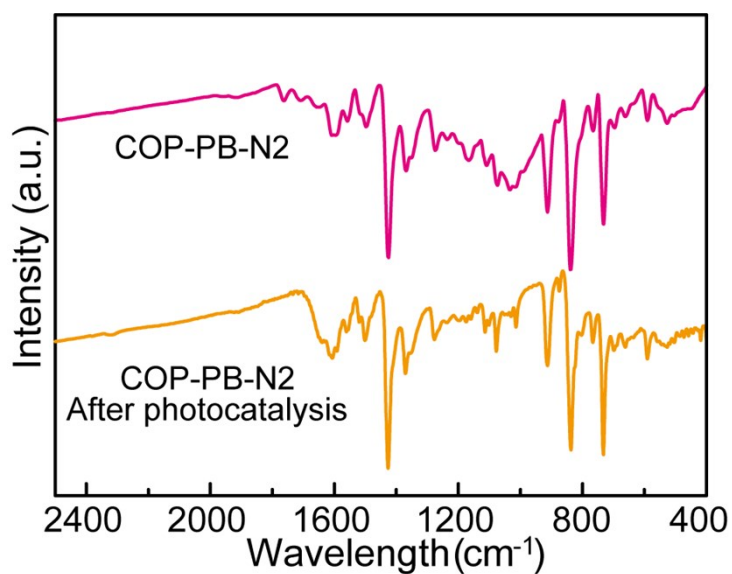


Figure S17. The FT-IR spectra of COP-PB-N2 before and after photocatalysis.

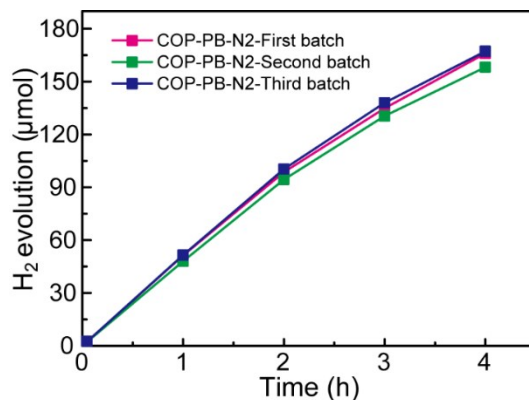


Figure S18. Hydrogen generation of COP-PB-N2 produced from different batches under visible light irradiation ( $\lambda \geq 400$  nm).

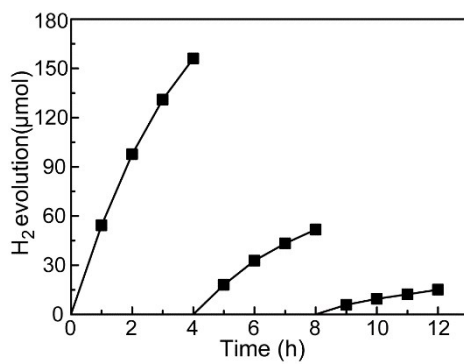


Figure S19. Photocatalytic cycle testing of COP-PB-N2.

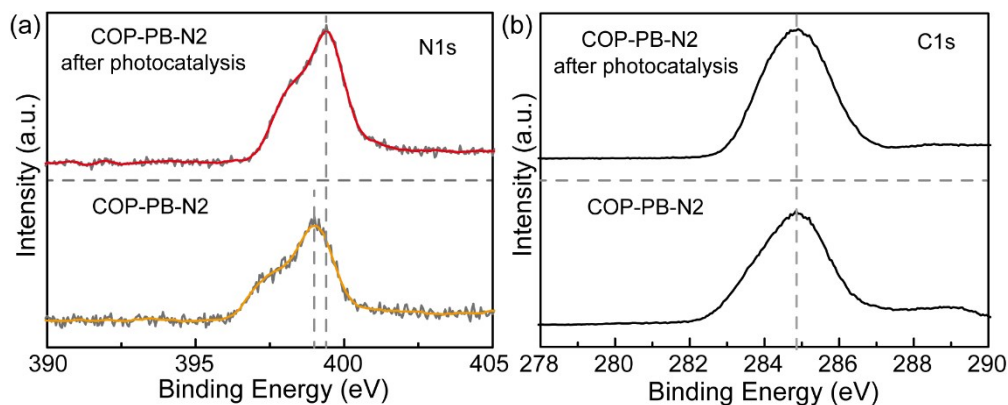


Figure S20. High resolution X-ray photoelectron spectroscopy (XPS) spectra of COP-PB-N2 before and after photocatalytic cyclic testing, (a) N1s; (b) C1s.

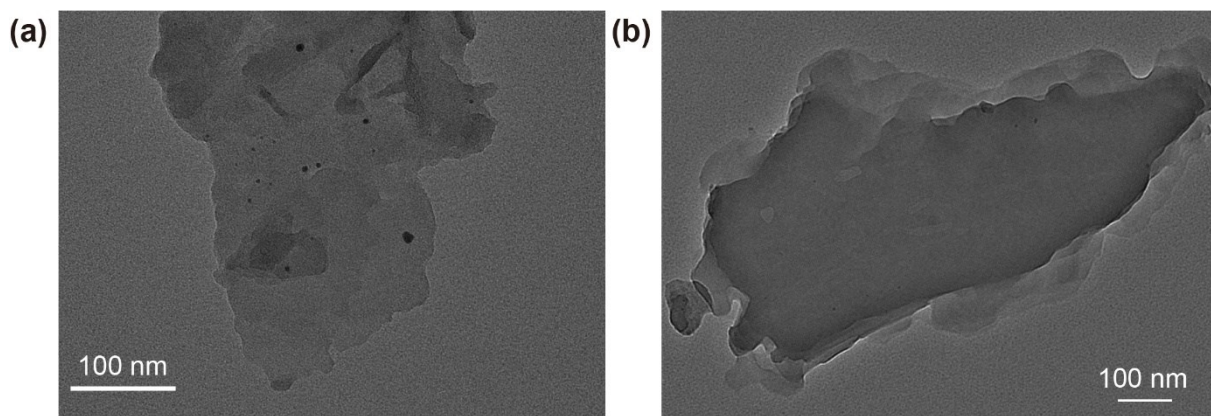


Figure S21. (a) TEM images of COP-PB-N2 before photocatalytic hydrogen evolution; (b) TEM images of COP-PB-N2 after photocatalytic hydrogen evolution.

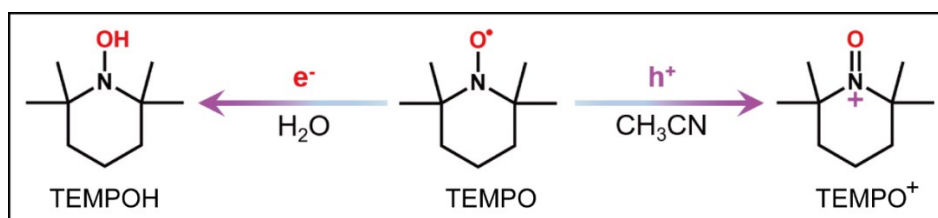


Figure S22. The mechanism image of detecting photo-excited electrons and holes via TEMPO-based EPR.

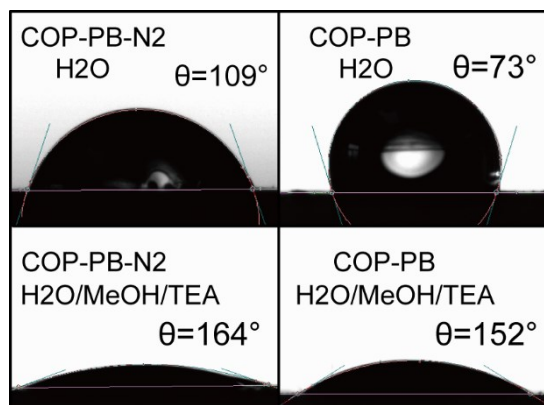


Figure S23. The contact angles image of COP-PB and COP-PB-N2 with water and H<sub>2</sub>O/MeOH/TEA mixture.

Table S1. The lifetimes of time-resolved transient PL decay of COP-PB and COP-PB-N2.

Photocatalyst	$\tau_1$ (ns)	$\tau_2$ (ns)	$\tau_3$ (ns)	$\tau_{av}$ (ns)
COP-PB	0.178 (53.64 %)	1.091 (40.91 %)	6.635 (5.45 %)	3.2
COP-PB-N2	0.190 (84.84 %)	1.450 (11.97 %)	8.513 (3.18 %)	4.3

The average lifetime ( $\tau_{av}$ ) was determined by the equation:

$$\tau = \frac{\sum_{i=1}^{i=n} a_i \tau_i^2}{\sum_{i=1}^{i=n} a_i \tau_i}$$

Table S2. The photocatalytic apparent quantum yield results of reported conjugated polymers.

Catalyst	Solvent	Irradiation	Polymer concentration (mg ml <sup>-1</sup> )	AQY (%)	Reference
COP-PB-N2	Water/MeOH/TEA	400 nm	1	35.5	This work
COP-PB-N2	Water/MeOH/TEA	400 nm	0.25	22.1	This work
SP-CMP	Water/MeOH/TEA	420 nm	1.11	0.23	S6
PFTBTA-PtPy	Water/ TEA	420 nm	0.06	0.27	S7
CP1	Water/AA/DMF	400 nm	0.18	0.77	S8
PFODTBT	Water/AA	420 nm	0.013	0.9	S9
TFPT-OCH3	Water/TEOA	405 nm	0.5	1.03	S10
PF2T	Water/MeOH/TEA	420 nm	0.5	1.17	S11
P12	Water/MeOH/TEA	420 nm	1	1.4	S12

OB-POP-3	Water/TEOA	420 nm	0.5	2	S13
CP-st	Water/NMP/AA	400 nm	0.17	2.2	S14
P7	Water/MeOH/TEA	420 nm	1.11	2.3	S15
Py-SO	Water/Et <sub>3</sub> N/MeOH	420 nm	0.33	3.28	S16
DBTD-CMP1	Water/TEOA	400 nm	0.5	3.3	S17
BBT- SC2NH2	Water/TEOA	420 nm	1	3.3	S18
P16PySO	Water/TEOA	450 nm	0.5	3.5	S19
P1	Water/TEOA	420 nm	/	3.58	S20
N-PDBT-O	Water/TEOA	420 nm	1	3.7	S21
B-BT-1,4	Water/TEOA	420 nm	0.5	4.02	S22
PySEO-2	Water/TEOA	400 nm	/	4.1	S23
PyDF	Water/TEOA	400 nm	0.25	4.5	S24
B-FOBT-1,4- E	Water/TEOA	420 nm	1	5.7	S25
F0.5CMP	Na <sub>2</sub> S/Na <sub>2</sub> SO <sub>4</sub>	420 nm	0.125	5.8	S26
PyDOBT-1	Water/TEOA	420 nm	0.5	6.1	S27
4-C2PN	Water/TEOA	420 nm	0.33	6.4	S28
P28	Water/MeOH/TEA	420 nm	1	6.7	S29
FSO-FS	Water/TEOA	420 nm	0.5	6.8	S30
CTF-BT/Th-1	Water/TEOA	420 nm	0.5	7.3	S31



PDBTSO	Water/TEOA	420 nm	0.1	8.4	S32
P-FSO	Water/TEOA	420 nm	0.5	8.5	S33
P10	Water/MeOH/TEA	420 nm	1	11.6	S34
S-CMP3	Water/MeOH/TEA	420 nm	1	13.2	S35
P10-e	Water/MeOH/TEA	420 nm	1	20.4	S36
P62	Water/MeOH/TEA	420 nm	1	15.1	S37
P64	Water/MeOH/TEA	420 nm	1	20.7	S37

**Note:** The AQY of 35.5% for COP-PB-N2 is achieved at the polymer concentration of 1 mg mL<sup>-1</sup> at 400 nm.

Table S3. The amount of Pd determined by ICP-MS.

Photocatalyst	Pd (wt %)
COP-PB	0.58
COP-PB-N2	0.12

Table S4. The raw data of energies for hydrogen evolution reaction energy profile.

Name	E <sub>DFT</sub> (eV)	T×S (eV) (298.25K)	ZPE (eV)
COP-PB-Site1	-226.4894	0.0021	0.3006
COP-PB-Site2	-226.5027	0.0015	0.3107
COP-PB-Site3	-226.4325	0.0020	0.3023
COP-PB-Site4	-226.2263	0.0016	0.3070
COP-PB-Site5	-225.7971	0.0019	0.2979
COP-PB-Site6	-226.8168	0.0018	0.3081
COP-PB-N2-Site1	-218.1600	0.0046	0.3233
COP-PB-N2-Site2	-217.0634	0.0017	0.3072

COP-PB-N2-Site3	-217.0567	0.0018	0.3062
COP-PB-N2-Site4	-216.8044	0.0016	0.3075
COP-PB-N2-Site5	-216.4982	0.0018	0.3008
COP-PB-N2-Site6	-217.2579	0.0019	0.3070
COP-PB-N1-Site1	-222.4656	0.0077	0.32779935
H <sub>2</sub>	-6.7703	0.4034	0.2785
COP-PB	-224.0274		
COP-PB-N1	-219.4984		
COP-PN-N2	-214.6512		

Table S5. Elemental analysis of the polymers.

Polymer	C (%)	H (%)	N (%)
COP-PB-N2	75.04	4.01	8.97
COP-PB	86.31	4.64	/

#### COP-PB

C001	0.7365800345081865	0.4831230463258294	0.7164095584755330
C002	0.6781996382401019	0.5430020380084315	0.7302675983804363
C003	0.5653731123026446	0.5455487611185674	0.7192913794046305
C004	0.5097595462717948	0.4855306071938443	0.7030728335592542
C005	0.5637912120527062	0.4198359906415661	0.7183027507616799
C006	0.6837027767705521	0.4233077528725673	0.7109662680443947
C007	0.5089092502198795	0.6081133463532922	0.7161152649236868
C008	0.4051783214495686	0.4885807141283678	0.6750991559028989
C009	0.3491183478566739	0.5517557154819173	0.6729942897803127
C010	0.4036759995650030	0.6109467862815521	0.6944420936867388
C011	0.2380933111096795	0.5522721998599422	0.6565177117341534
C012	0.1835750788566628	0.4932645237219759	0.6420434835608972
C013	0.2433271325130093	0.4332406487740883	0.6332682909595775
C014	0.3512158293805001	0.4308080047381750	0.6499144188382786
C015	0.0660980006341987	0.4894442833235146	0.6524554091723260
C016	0.0310114302708087	0.4386545714051877	0.6959405102426075
C017	0.9928760110321733	0.5385039018837290	0.6310342308469643
C018	0.9248570626223582	0.4375180438348067	0.7189536832291452
C019	0.8862936765818503	0.5370812504857696	0.6539494386674818
C020	0.8518530791304997	0.4868291666295264	0.6981047939502929
H001	0.1922739278696568	0.5986956655766633	0.6622919299966981
H002	0.5524135454264538	0.6534304738375809	0.7307062746255326
H003	0.7227084509835748	0.5890867914463485	0.7404589570818558
H004	0.5313665458608483	0.3788009461664430	0.6876956069276901
H005	0.7285026723781058	0.3780369110242319	0.6980797267674674
H006	0.3596460717740229	0.6583407924287243	0.6931813505579072
H007	0.2011459229071662	0.3884114110156176	0.6161398326911893
H008	0.3951843903522061	0.3838057403483930	0.6448638009903931
H009	0.0897898586815060	0.4021619834578374	0.7142420055161978
H010	0.0198584705062430	0.5774066767004697	0.5965305525170663
H011	0.8981891145734409	0.3991567277144341	0.7541361355001754
H012	0.8276384036312123	0.5740625017130654	0.6364068226722495

H013 0.5420641046867161 0.4054842965074883 0.7705539130343197

**COP-PB-N1**

C001 0.7377802493263488 0.4880322959952395 0.7178100724131582  
C002 0.6813950129111603 0.5493569416517659 0.7270539712912623  
C003 0.5689415340465942 0.5516120228645320 0.7160919716792336  
C004 0.5141134084862031 0.4908132041969466 0.7020239102832164  
C005 0.6805605866605617 0.4292476915505503 0.7132738253707913  
C006 0.5069737712437359 0.6122048585366571 0.7138687560416273  
C007 0.4073507320559884 0.4893413747782489 0.6776747434132346  
C008 0.3472740017837737 0.5508663321655121 0.6765416326746632  
C009 0.3996678577594750 0.6115192294817149 0.6957124287924898  
C010 0.2361936132237759 0.5480164777070371 0.6613989564510021  
C011 0.1853335173153354 0.4872482065990695 0.6483260787437928  
C012 0.2483563918326936 0.4283194311242866 0.6411119429166874  
C013 0.0679640312948351 0.4830007709033097 0.6566947777177674  
C014 0.0282952267566898 0.4333881884461519 0.7001414417818594  
C015 0.9979835742185301 0.5331060557123237 0.6333249447329479  
C016 0.9217768085714511 0.4354960053634187 0.7223374165248870  
C017 0.8912931970052185 0.5350355896384968 0.6552175396564124  
C018 0.8527153414928108 0.4866521527640657 0.7002937364599831  
C019 0.3572974093626158 0.4292467786178804 0.6553464712749530  
H001 0.1873597644329124 0.5933521964822006 0.6662517390338110  
H002 0.5476848427906233 0.6589566637814670 0.7267564389960626  
H003 0.7267689214809536 0.5952893099858088 0.7360867676144309  
H004 0.7189717600056156 0.3807477152178933 0.7062961956616221  
H005 0.3521907930815900 0.6576706534901291 0.6955129647095930  
H006 0.2085871615921633 0.3821869457290177 0.6253088383562897  
H007 0.0843728349156336 0.3959593053736512 0.7197881452869765  
H008 0.0283866076237871 0.5706230092407125 0.5983576169226765  
H009 0.8924296246505179 0.3988779845272319 0.7585822835559384  
H010 0.8353978327667164 0.5730651095400034 0.6365166007011354  
H011 0.4047033452459701 0.3835760016417211 0.6484053654615991  
H012 0.5275426627930671 0.3880193447676987 0.7067884927341055  
N001 0.5698409138321452 0.4312000136091072 0.7114488660036642

**COP-PB-N2**

C001 0.7355792912820149 0.4854950918957925 0.7103123027557743  
C002 0.6834990803096304 0.5479226219855988 0.7224809630150020  
C003 0.5705032693786336 0.5524976582079049 0.7158592503123984  
C004 0.5124884283009052 0.4927977275297266 0.7031570874560913  
C005 0.6748081708503051 0.4279888560296286 0.7042728118100996  
C006 0.5100122979121764 0.6139230399904747 0.7155087291712192  
C007 0.4031682131860421 0.4927734135221939 0.6840960220327830  
C008 0.3456927726882100 0.5548217703311735 0.6820594477483937  
C009 0.4019399093882896 0.6149513403289504 0.6990957432816671  
C010 0.2352116280362253 0.5513441918275603 0.6666641959740502  
C011 0.1873710822074415 0.4890626616603271 0.6550487298654417  
C012 0.2546624330545413 0.4315703030559490 0.6531857836975234  
C013 0.0699208275243421 0.4821646256658099 0.6577764857338408  
C014 0.0267809100623353 0.4306990136904076 0.6976582279602468  
C015 0.0006470365118219 0.5317040722252955 0.6322140658473643  
C016 0.9181134499571613 0.4310908560040119 0.7154918903646106  
C017 0.8919062320104061 0.5320619944779708 0.6499000253097336  
C018 0.8503709201291869 0.4826927914465671 0.6929188170784357  
H001 0.1851571039240412 0.5963991587444113 0.6684566048613263  
H002 0.5530241921555472 0.6602395683254301 0.7271395731224075

H003	0.7323899075914326	0.5925721720756130	0.7310294659376382
H004	0.7107494041375446	0.3791868966498058	0.6947048638906921
H005	0.3570511795700213	0.6620827199407628	0.6983492895575907
H006	0.2190627275238484	0.3832042537777838	0.6398688000711985
H007	0.0812780960675639	0.3931979765280360	0.7187735533643860
H008	0.0332296257622247	0.5701625260656868	0.5990684532241559
H009	0.8862194966382333	0.3933100225033499	0.7496524580509742
H010	0.8371460657989687	0.5701483699815100	0.6300902476827730
H011	0.5156435893970794	0.3923775316758906	0.6930017281951990
N001	0.5648397537509098	0.4317436803217660	0.7053008625052186
N002	0.3591252628929027	0.4322003075346217	0.6674885331217908

## References

- S1 Y. Liu, Z. Liao, X. Ma and Z. Xiang, *ACS Appl. Mater. Interf.*, 2018, **10**, 30698-30705.
- S2 Y. Liu and Z. Xiang, *ACS Appl. Mater. Interf.*, 2019, **11**, 41313-41320.
- S3 G. Kresse, *Phys. Rev. B*, 1996, **54**, 11169-11186.
- S4 K. B. John P. Perdew, M. Ernzerhof, *Phys. Rev. Lett.*, 1996, **77**, 3865-3868.
- S5 G. Kresse, *Phys. Rev. B*, 1999, **59**, 1758-1775.
- S6 R. S. Sprick, B. Bonillo, M. Sachs, R. Clowes, J. R. Durrant, D. J. Adams and A. I. Cooper, *Chem. Commun.*, 2016, **52**, 10008-10011.
- S7 C. L. Chang, W. C. Lin, C. Y. Jia, L. Y. Ting, Y. Q. Yang, Y. H. Chan, W. S. Wang, C. Y. Lu, P. Y. Chen and H. H. Chou, *Appl. Catal. B-Environ.*, 2020, **268**, 118436.
- S8 W. Y. Huang, Z. Q. Shen, J. Z. Cheng, S. Y. Liu, *J. Mater. Chem. A.*, 2019, **7**, 24222-24230.
- S9 P. B. Pati, G. Damas, L. Tian, D. L. A. Fernandes, L. Zhang, I. B. Pehlivan, T. Edvinsson, C. M. Araujo and H. Tian, *Energy Environ. Sci.*, 2017, **10**, 1372-1376.
- S10 K. Yu, S. Bi, W. Ming, W. Wei, Y. Zhang, J. Xu, P. Qiang, F. Qiu, D. Wu and F. Zhang, *Poly. Chem.*, 2019, **10**, 3758-3763.
- S11 L. Y. Ting, J. Jayakumar, C. L. Chang, W. C. Lin, M. H. Elsayed and H. H. Chou, *J. Mater. Chem. A.*, 2019, **7**, 22924-22929.
- S12 R. S. Sprick, C. M. Aitchison, E. Berardo, L. Turcani, L. Wilbraham, B. M. Alston, K. E. Jelfs, M. A. Zwijnenburg and A. I. Cooper, *J. Mater. Chem. A.*, 2018, **6**, 11994-12003.
- S13 S. Bi, W. Zhang, Y. He, X. C. Wang, F. Zhang, *Adv. Funct. Mater.*, 2017, **27**, 3146-3124.
- S14 J. Z. Cheng, G. Liao, Z. Q. Shen, Z. R. Tan, Y. Q. Xing, S. Y. Liu, *J. Mater. Chem. A.*, 2020, **8**, 5890-5899.
- S15 R. S. Sprick, B. Bonillo, R. Clowes, P. Guiglion, N. J. Brownbill, B. J. Slater, F. Blanc, M. A. Zwijnenburg, D. J. Adams and A. I. Cooper, *Angew. Chem. Int. Ed.*, 2016, **55**, 1824-1828.
- S16 C. Dai, S. Xu, W. Liu, X. Gong, M. Panahandeh-Fard, Z. Liu, D. Zhang, C. Xue, K. P. Loh and B. Liu, *Small.*, 2018, **14**, 1801839.
- S17 Z. Wang, X. Yang, T. Yang, Y. Zhao, F. Wang, Y. Chen, J. H. Zeng, C. Yan, F. Huang and J. X. Jiang, *ACS Catal.*, 2018, **8**, 8590-8596.
- S18 X. Wang, X. Zhao, W. Dong, X. Zhang, Y. Xiang, Q. Huang and H. Chen, *J. Mater. Chem. A.*, 2019, **7**, 16277-16284.
- S19 C. Cheng, X. Wang and F. Wang, *Appl. Surf. Sci.*, 2019, **495**, 143537.
- S20 J. Yu, X. Sun, X. Xu, C. Zhang and X. He, *Appl. Catal. B-Environ.*, 2019, **257**, 117935.
- S21 X. Wang, B. Chen, W. Dong, X. Zhang, Z. Li, Y. Xiang and H. Chen, *Macromol. rapid. commun.*, 2018, **40**, 1800494.
- S22 C. Yang, B. C. Ma, L. Zhang, S. Lin, S. Ghasimi, K. Landfester, K. A. Zhang and X. Wang, *Angew. Chem. Int. Ed.*, 2016, **55**, 9202-9206.
- S23 C. Shu, Y. Zhao, C. Zhang, X. Gao, W. Ma, S. B. Ren, F. Wang, Y. Chen, J. H. Zeng and J. X. Jiang, *ChemSusChem.*, 2020, **13**, 369-375.
- S24 X. Gao, C. Shu, C. Zhang, W. Ma, S. B. Ren, F. Wang, Y. Chen, J. H. Zeng and J. X. Jiang,

- J. Mater. Chem. A.*, 2020, **8**, 2404-2411.
- S25 Y. Xiang, X. Wang, L. Rao, P. Wang, D. Huang, X. Ding, X. Zhang, S. Wang, H. Chen and Y. Zhu, *ACS Energy Lett.*, 2018, **3**, 2544-2549.
- S26 V. S. Mothika, P. Sutar, P. Verma, S. K. Pati and T. K. Maji, *Chem.*, 2019, **25**, 3867-3874.
- S27 Y. Zhao, W. Ma, Y. Xu, C. Zhang, Q. Wang, T. Yang, X. Gao, F. Wang, C. Yan and J. X. Jiang, *Macromolecules.*, 2018, **51**, 9502-9508.
- S28 G. Zhang, W. Ou, J. Wang, Y. Xu, D. Xu, T. Sun, S. Xiao, M. Wang, H. Li, W. Chen and C. Su, *Appl. Catal. B-Environ.*, 2019, **245**, 114-121.
- S29 R. S. Sprick, L. Wilbraham, Y. Bai, P. Guiglion, A. Monti, R. Clowes, A. I. Cooper and M. A. Zwijnenburg, *Chem. Mater.*, 2018, **30**, 5733-5742.
- S30 Z. A. Lan, G. Zhang, X. Chen, Y. Zhang, K. A. I. Zhang and X. Wang, *Angew. Chem. Int. Ed.*, 2019, **58**, 10236-10240.
- S31 W. Huang, Y. Hu, and Y. Li, *Angew. Chem. Int. Ed.*, 2019, **58**, 8676-8680.
- S32 G. Shu, Y. Li, Z. Wang, J. X. Jiang and F. Wang, *Appl. Catal. B-Environ.*, 2020, **261**, 118230.
- S33 Z. A. Lan, W. Ren, X. Chen, Y. Zhang and X. Wang, *Appl. Catal. B-Environ.*, 2019, **245**, 596-603.
- S34 M. Sachs, R. S. Sprick, D. Pearce, S. A. J. Hillman, M. A. Zwijnenburg, J. Nelson, J. R. Durrant and A. I. Cooper, *Nat Commun.*, 2018, **9**, 4968-4979.
- S35 R. S. Sprick, Y. Bai, A. A. Y. Guilbert, M. Zbiri, C. M. Aitchison, L. Wilbraham, Y. Yan, D. J. Woods, M. A. Zwijnenburg and A. I. Cooper, *Chem. Mater.*, 2018, **31**, 305-313.
- S36 Catherine M. Aitchison, R. S. Sprick and A. I. Cooper, *Journal of Materials Chemistry A*, 2019, **7**, 2490-2496.
- S37 Y. Bai, L. Wilbraham, B. J. Slater, M. A. Zwijnenburg, R. S. Sprick and A. I. Cooper, *J. Am. Chem. Soc.*, 2019, **141**, 9063-9071.